Title

Comparison of ground motion attributes from 2011 Tohoku-oki mainshock and two subsequent events

Journal

Proc. 10th International Conf. on Urban Earthquake Engin., 10(1)

Authors

Kishida, Tadahiro
Stewart, Jonathan P
Graves, Robert W
et al.

Publication Date

2013-03-02

10CUEE CONFERENCE PROCEEDINGS
10th International Conference on Urban Earthquake Engineering
March 1-2, 2013, Tokyo Institute of Technology, Tokyo, Japan

COMPARISON OF GROUND MOTION ATTRIBUTES FROM 2011 TOHOKU-OKI MAINSHOCK AND TWO SUBSEQUENT EVENTS

Tadahiro Kishida[1)], Jonathan P. Stewart[2)], Robert W. Graves[3)], Saburoh Midorikawa[4)], Hiroyuki Miura[5)], Yousef Bozorgnia[1)] , and Kenneth W. Campbell[6)]

1) Post-Doctoral Scholar (TK) and Executive Director (YB), Pacific Earthquake Engineering Research Center, Berkeley, CA, USA
2) Professor and Chair, Dept. of Civil & Environmental Engineering, Univ. of California, Los Angeles, CA, USA
3) Seismologist, US Geological Survey, Pasadena, CA, USA
4) Professor, Tokyo Institute of Technology, Japan
5) Associate Professor, Hiroshima University, Japan
6) Vice President, EQECAT Inc, Beaverton OR, USA

tkishida@berkeley.edu, jstewart@seas.ucla.edu, rwgraves@usgs.gov, ,
smidorik@enveng.titech.ac.jp, hmiura@hiroshima-u.ac.jp, yousef@berkeley.edu, kcampbell@eqecat.com

Abstract: The M_w 9.0 Tohoku-oki Japan earthquake and many of its subsequent aftershocks and triggered events were very well recorded, providing opportunity for detailed study of source, path, and site effects. In previous work, we utilized mainshock data to demonstrate faster attenuation with distance in backarc than in forearc regions, positive event terms for high frequency intensity measures for multiple ground motion prediction models, and minimal scaling of site amplification with V_{s30} at high frequencies. In this paper, we consider two subsequent events, one M_w 6.7 on the plate interface that ruptured in the mainshock and one M_w 6.3 inland from the volcanic front, to examine if similar ground motion features are apparent from these data sets. We continue to find evidence for the divergence in attenuation rate in forearc and backarc regions, despite the fact that the events are located on opposite sides of the volcanic front. The site response for these events does not appear to follow previously observed patterns for Japan, being relatively similar to V_{s30}-scaling in active crustal regions generally.

1. INTRODUCTION

The M_w 9.0 Tohoku-oki earthquake occurred on March 11 2011 along the plate boundary off the Pacific Coast of Japan. In prior work (Stewart et al., 2013), we reviewed the mainshock source solutions and selected a representative source model for engineering application; we described the uniform ground motion processing applied to approximately 2000 available triaxial accelerograms; and we described the results of data analysis to investigate source, path and site effects. For short period ground motion intensity measures, we found faster attenuation with distance in backarc than in forearc regions, positive event terms for multiple ground motion prediction models at short periods, and minimal scaling of site amplification with V_{s30}. Many of these effects disappeared at long periods.

Many of these observations are of substantial practical significance for ground motion prediction, and therefore there is interest in seeing if they are repeatable. This paper represents a first step in this direction. We select two well recorded events that occurred subsequent to the mainshock, one M_w 6.7 on the same plate interface that ruptured in the mainshock and one M_w 6.3 inland from the volcanic front. Identical data processing procedures are applied to these recordings as were used for the mainshock. Our objective is to see if similar ground motion features are apparent from these data sets as were found from the mainshock.

2. SELECTED EVENTS AND AVAILABLE DATA

We selected two events from the Japan Meteorological Assoc. (JMA) web site (http://www.seisvol.kishou.go.jp/eq/sourceprocess/). Attributes of the two events are given in Table 1. We refer to the 12 March 2011 event as 'crustal' and the 23 June 2011 event as 'interface.' As shown in Figure 1, the crustal event occurred in the backarc region. It had a reverse-slip mechanism and a shallow focal depth (8 km). The interface event occurred near the northwest corner of the mainshock fault plane (Fig. 1). It had a reverse-slip mechanism along a 17 deg. westward dipping fault plane and a focal depth of 36 km, which are consistent with rupture along the plate interface. In addition, this event is located close to the 03-11-2011 M_w 7.4 aftershock (Fig 1), which is also inferred to have rupture at the plate interface.

Table 1. Attributes of selected events

Date	M_w	Top-Ctr Lat, Long	Depth to top (km)	Length, width (km)	Strike / dip (°)
3/2011	6.3	37.051, 138.532	4.4	12, 12	26 / 32
6/2011	6.7	39.982, 142.588	36	18, 12	185/17

There are hundreds of well recorded events following the Tohoku mainshock. Our reasons for selecting these specific events were:

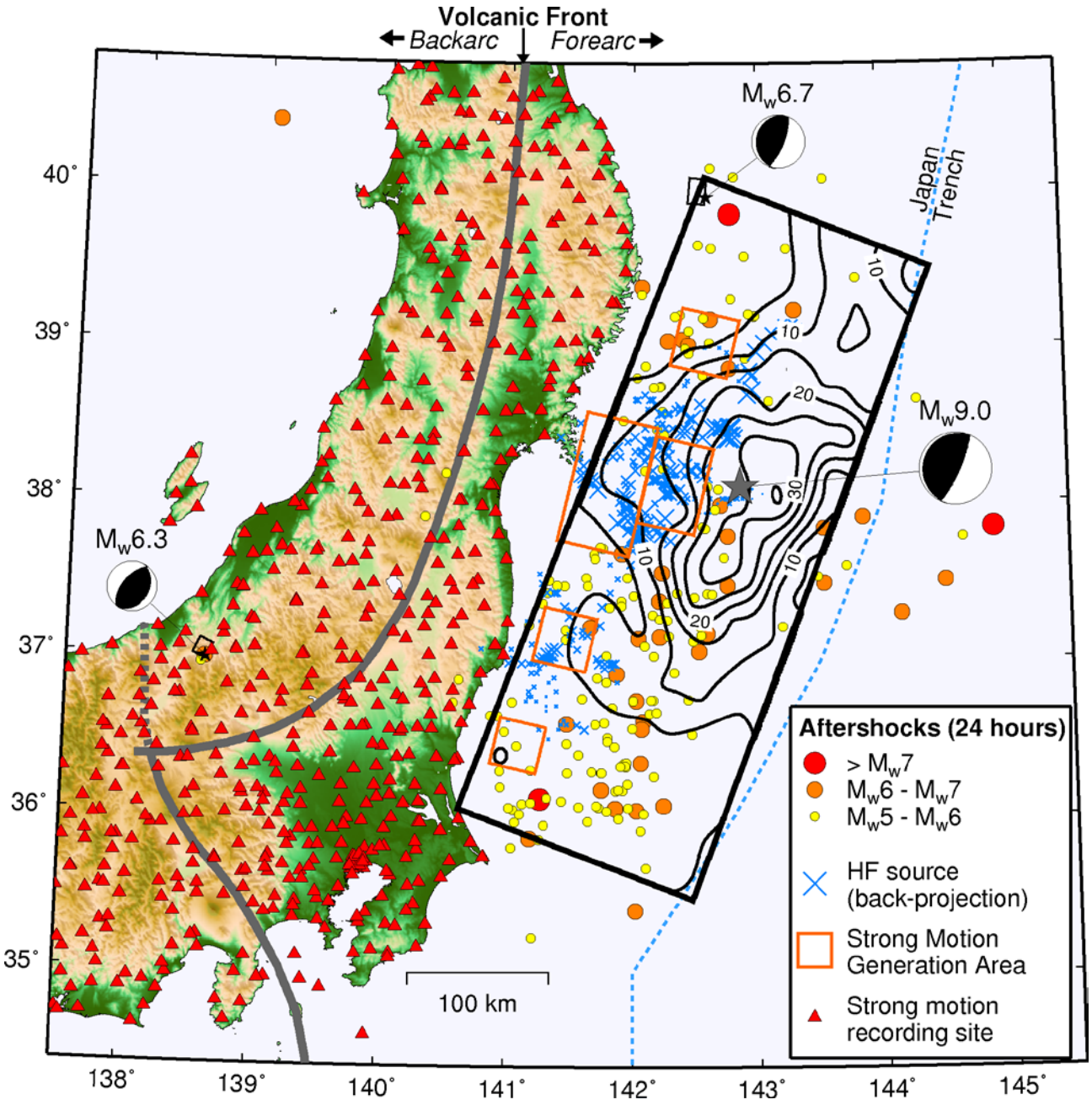

Figure 1. Map view showing surface projections of two selected triggered events for this study (Mw 6.3 crustal event and Mw 6.7 interface event) along with various attributes of mainshock fault model selected by Stewart et al. (2013), which is derived from Yokota et al. (2011). Mainshock fault attributes shown are the Strong Motion Generation Areas of Kurahashi and Irikura (2011) (orange rectangles) and the high-frequency back-projection source locations of Meng et al. (2011) (blue crosses). Contours indicate slip (m) for the Yokota et al. rupture model. Colored circles show aftershocks within the first 24 hours following the mainshock. Dashed blue line indicates location of Japan Trench and the gray star is the JMA epicenter of the mainshock. The red triangles denote the locations of some of the strong motion recording sites considered in our analysis (additional stations were considered beyond the limits of the map).

1. *Location relative to plate boundary.* We sought events on, and inboard from, the plate boundary. This was to see if the forearc/backarc path effects are similar for waves travelling principally in a forearc-to-backarc direction (source to instruments) or vice-versa. We are also interested in event-term trends for these earthquakes relative to the mainshock.
2. *Recordings*. We sought events with numerous uniformly processed recordings using standard Pacific Earthquake Engineering Research (PEER) procedures (Darragh et al., 2004; Chiou et al., 2008) as of 12/2012. The crustal & interface events produced 520 & 472 records.
3. *Magnitude*. We sought events with similar magnitudes.

For the crustal event, we took the fault plane solution of Nagumo (2012). We examined several other fault plane solutions for this event from the JMA web site (http://www.seisvol.kishou.go.jp/eq/sourceprocess/event/201103120359near.pdf, last accessed Dec 2012) and NIED web site (http://cais.gsi.go.jp/YOCHIREN/report/kaihou86/07_04.pdf, last accessed Dec 2012). The Nagumo model was selected because its fault plane solution is most clearly documented. For the interface event, we take the only available fault plane solution, which is from the JMA web site (http://www.seisvol.kishou.go.jp/eq/sourceprocess/ event/20110623near.pdf, last accessed Jan 2013). Both of the selected fault planes are shown in Figure 1.

For both events, we obtained available ground motion records from the Knet and Kik-net arrays at the NIED web site (http://www.kyoshin.bosai.go.jp/kyoshin/, last accessed Dec 2012). A total of 554 and 641 three-component uncorrected digital accelerograms were selected for the crustal and interface events, respectively. Sponsored by the PEER center, those motions were processed by Pacific Engineering and Analysis following PEER/NGA protocols (Darragh et al., 2004; Chiou et al., 2008), which include selection of record-specific corner frequencies to optimize the usable frequency range. For Kik-net sites, only data from the ground surface stations are considered.

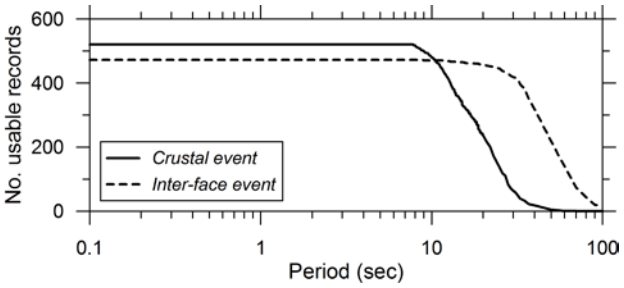

Figure 2. Number of usable two-component horizontal records as function of spectral period for the two data sets

The most important filter is the low-cut filter, which removes low frequency noise effects. We take the minimum usable frequency as $1.25 \times f_{HP}$, where f_{HP} is the high-pass (equivalent to low-cut) corner frequency used in the processing. Using the filtered records, we computed the intensity measures of peak acceleration (PGA), peak velocity (PGV), and pseudo-acceleration response spectra at a range of periods between 0.01 and 10.0 sec. Figure 2 presents the number of usable recordings as a function of period. A usable recording for period T is defined as having both horizontal components with $T < 1/(1.25\ f_{HP})$. The data set is seen to fall off for periods beyond about 10-30 sec.

3. DATA ANALYSIS

3.1 Analysis Procedures

The data analysis follows the same procedures described in Stewart et al. (2013), and hence is described here only briefly. Essentially, we compute total residuals (data minus model in natural log units) using an applicable ground motion prediction equation (GMPE). In this case, we use the Zhao et al. (2006) GMPE. Event terms are computed using the mean of total residuals for conditions where distance attenuation bias is judged to not significantly contaminate the results. Distance attenuation trends are evaluated from the trends of residuals with distance.

A second set of residuals is computed as the difference between data and the GMPE for rock conditions (described in Stewart et al., 2013). These residuals are used to evaluate the scaling of ground motions with the time averaged shear wave velocity in the upper 30 m of the site (V_{s30}).

3.2 Distance Attenuation

Figure 3 shows RotD50 values (i.e, median of single-azimuthal ground motions; Boore, 2010) for PGA, 0.1 s, 1.0 s, and 3.0 s pseudo-acceleration (PSA) at 5% damping versus rupture distance. Also shown in Figure 3a are medians (μ) and medians ± one intra-event standard deviation (ϕ_{ln}) for the ZEA (Zhao et al.) 2006 GMPE for the site category having $V_{s30} \approx 300$ m/s. Figure 4 shows total residuals versus rupture distance. Forearc and backarc sites are distinguished in both Figures 3 and 4.

Several significant trends are evident from Figure 3 and 4. The crustal event occurs in the backarc region and produced backarc recordings from nearly zero distance to large distance. Forearc recordings begin at about 80 km. As shown by the binned median residuals, the forearc recordings have an upward shift relative to the backarc, which is consistent with previously observed trends of faster distance attenuation in backarc than forearc regions (Ghofrani and Atkinson, 2011). This is generally consistent with what we saw with the Tohoku mainshock, but interestingly in this case, the waves are crossing the volcanic front in opposite directions.

The interface event has forearc recordings starting at around 60 km and backarc recordings beginning at about 120 km. Backarc residuals have a clear downward shift relative to the forearc, which is the same trend observed with the Tohoku mainshock data (Ghofrani and Atkinson, 2011; Skarlatoudis and Papazachos, 2012; Stewart et al 2013). Hence, the apparent differences in anelastic attenuation rate in forearc and backarc regions appear to be stable across events and source locations (relative to volcanic front).

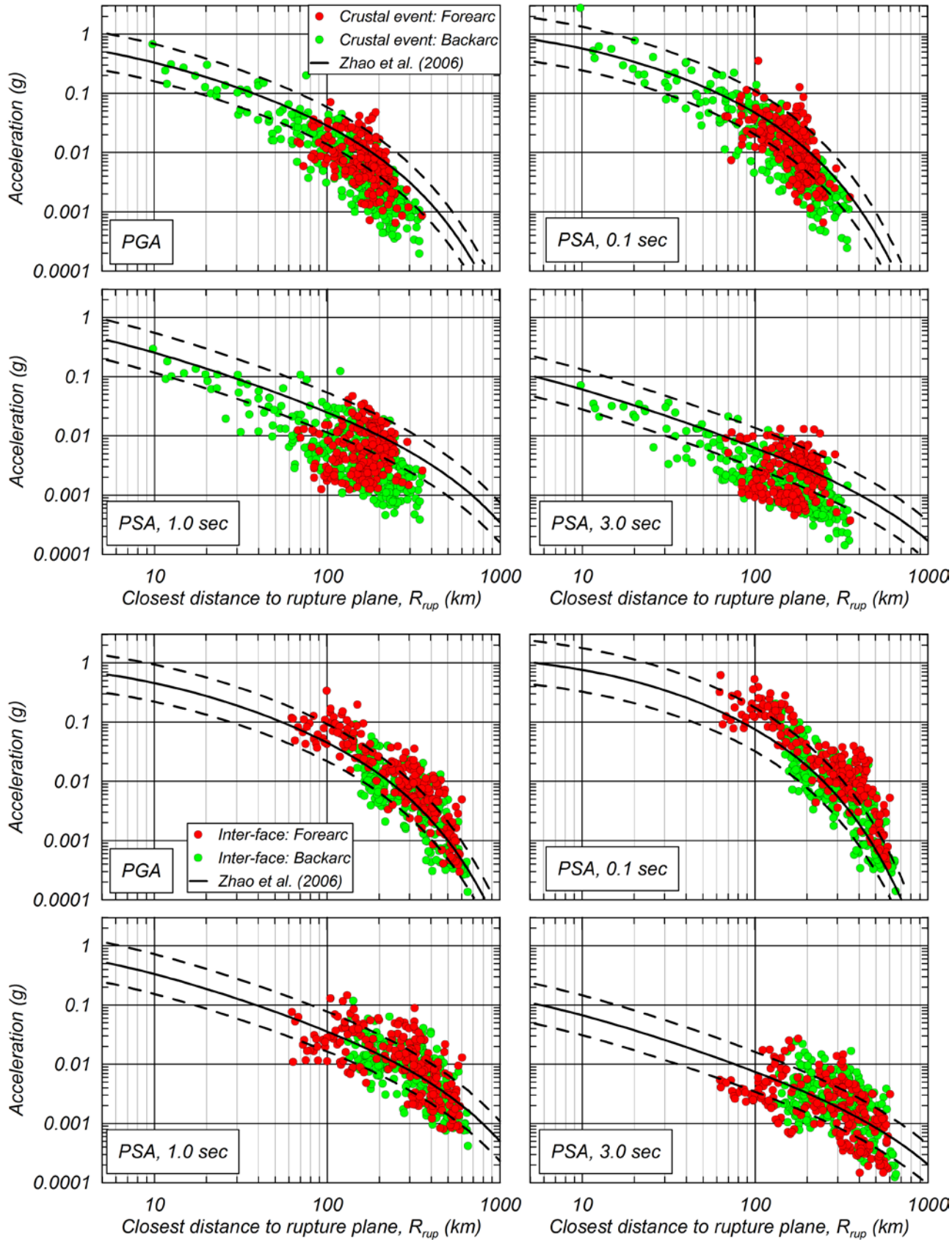

Figure 3. Ground motion intensity measures plotted against distance for crustal (top) and interface (bottom) triggered events. Backarc and forearc records shown with separate symbols. Zhao et al. 2006 GMPE shown for soil site condition.

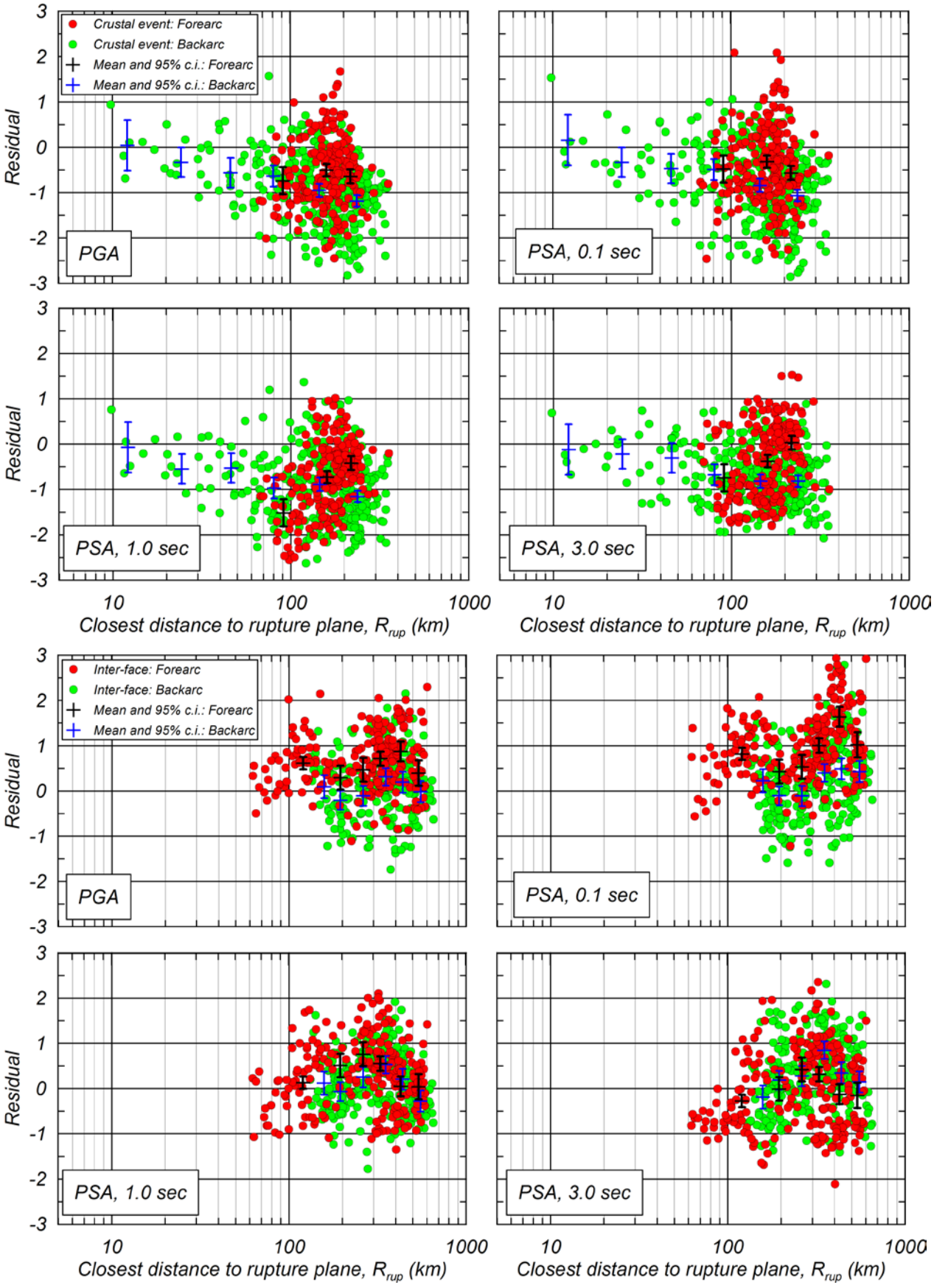

Figure 4. Distance-dependence of total residuals for crustal (top) and interface (bottom) events relative to ZEA 2006 GMPE.

3.3 Event Terms

As shown in Figure 4, in most cases the residuals are not centered at zero ordinate, indicating systematic misfits of the GMPE relative to the data. Since the events are well recorded, this bias is practically equivalent to an event term as would be calculated from a mixed-effects regression (e.g., Abrahamson and Youngs, 1992). Non-zero event terms (η) are typical; what is of interest is to see if the event terms are consistent with event-to-event scatter (represented by event term standard deviation τ) as observed from previous earthquakes. Figure 5 shows event terms, calculated using the following data for the two earthquakes:

1. For the crustal event, we use a combination of backarc recordings with closest distance (R_{rup}) < 70 km and forearc to R_{rup} < 250 km. We include the close-distance backarc records because the distance attenuation is dominated by geometric spreading in that region.
2. For the interface event, we use forearc recordings with R_{rup} < 250 km.

Event terms are taken as median residuals for the ZEA 2006 GMPE as a function of spectral period. Also shown in Figure 5 are the $\pm$ τ model (inter-event standard deviation) from ZEA 2006. We note that the mainshock and interface event terms have a similar trend with period, whereas the crustal event is different because of an increase at long period. One possible explanation for this is stronger surface waves excited by the shallow crustal event compared to the lack of surface waves for the relatively deep interface event. These surface waves would be more pronounced at the longer periods due to the higher attenuation of shorter periods in the shallow crust. Analyses of additional events are needed to determine whether these effects are accidental or systematic.

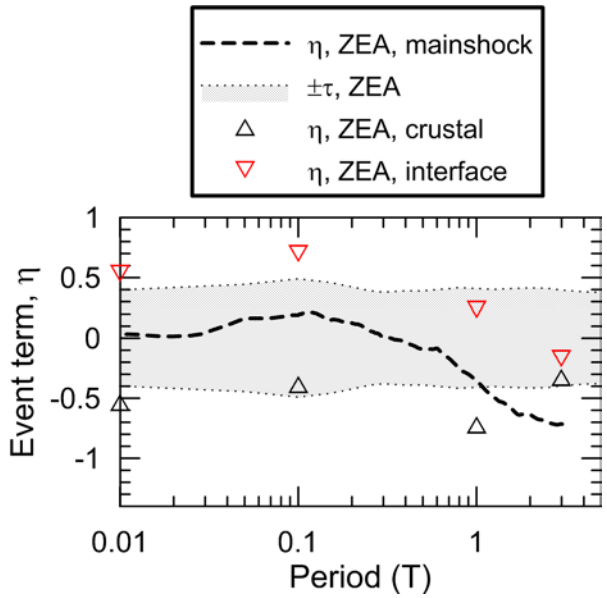

Fig. 5. Estimated event terms of Tohoku-oki mainshock and two triggered events relative to the ZEA 2006 GMPE. Also shown is the ZEA inter-event standard deviation (τ).

3.4 Site Response

A meaningful analysis of site effects from these data sets is complicated by the significant distance attenuation misfits identified in Section 3.2, which cause large non-zero residuals for reasons unrelated to site response. Accordingly, for the analysis of site effects, we use the subset of data used for event term computations (described in Section 3.3), for which distance attenuation trends are relatively well-matched by the ZEA GMPE. We use intra-event reference site residuals, which are total reference site residuals corrected to zero mean through subtraction of the event term (details in Stewart et al. 2013).

Figure 6 shows the trends of ZEA 2006 reference site residuals for the crustal event against V_{s30} for the intensity measures of PGA and PSA at 0.1, 1.0, and 3.0 sec. A log-linear regression is also shown.

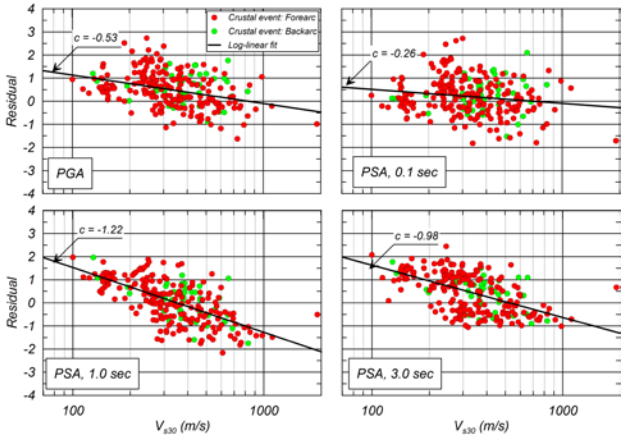

Fig. 6. Reference rock residuals of crustal event using ZEA 2006 GMPE for rock site conditions, showing scaling of site factors with V_{s30}.

Figure 7 shows the slopes of the fit lines (denoted as c) for both events against trends presented previously for the Tohoku mainshock and a representative model for active crustal regions (ACRs; Choi and Stewart, 2005). The slopes from these events differ from those for the mainshock at short periods, having stronger V_{s30} scaling. These differences may be influenced by nonlinearity.

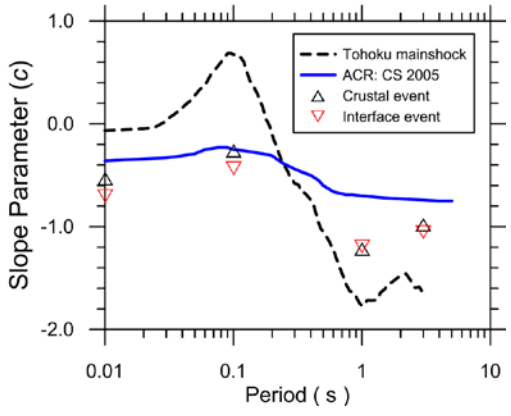

Fig. 7. V_{s30}-scaling of rock residuals (c parameter) from mainshock, subsequent events, and ACR model

4. CONCLUSIONS

In a separate paper investigating the attributes of the Tohoku-oki mainshock data (Stewart et al., 2013), we found important attributes of the ground motions that have substantial practical importance for seismic hazard analysis. Among those attributes were: (*i*) faster anelastic attenuation in the backarc region as compared to the forearc region; (*ii*) positive event terms at short periods that decrease as period increases; and (*iii*) scaling of site amplification with V_{s30} that is substantially reduced from that in active crustal regions at short periods but enhanced at long periods (weaker and stronger V_{s30}-scaling, respectively). We note here that the analysis of site effects from the Tohoku mainshock did not consider nonlinearities.

In this paper, we examine the repeatability of these effects using an admittedly small data set of two events subsequent to the mainshock – one a crustal event in the backarc region and one occurring at the plate interface on the mainshock fault plane. Both events are well recorded and the data was uniformly processed using standard PEER procedures in the same manner as the mainshock data.

We find the variable anelastic attenuation rates to be repeatable, even though one of the considered events occurred on the backarc side of the volcanic front. This is perhaps our most significant finding in this paper. The interface event terms follow a similar form to those from the mainshock, whereas the crustal event shows a different pattern at long periods, but we cannot draw statistically significant inferences from so few earthquakes. The V_{s30}-scaling from these events was much stronger at short periods than had been observed in the mainshock, but relatively consistent at long periods. The differences at short period may be a result of nonlinearity, but further study will be required to understand these differences.

Acknowledgements:

Partial supports for this work to PEER is provided by the USGS/NEHRP and FM Global, and which are gratefully acknowledged.

References:

Abrahamson, NA and RR Youngs (1992). A stable algorithm for regression analyses using the random effects model, *Bull. Seismol. Soc. Am.*, 82, 505–510.

Boore, DM (2010). Orientation-independent, nongeometric-mean measures of seismic intensity from two horizontal components of motion, *Bull. Seismol. Soc. Am.*, 100, 1830 – 1835.

Chiou, B, R Darragh, N Gregor, and WJ Silva (2008), NGA project strong-motion database. *Earthquake Spectra*, 24(1), 23–44.

Choi, Y. and Stewart, J.P. (2005). Nonlinear site amplification as function of 30 m shear wave velocity, *Earthquake Spectra*, 21 (1), 1-30.

Darragh, R, WJ Silva, and N Gregor (2004). Strong motion record processing for the PEER center, Proc. Workshop on Strong Motion Record Processing, Richmond, CA, May 26-27, 2004 (http://www.cosmos-eq.org/recordProcessingPapers.html).

Ghofrani, H and GM Atkinson (2011). Forearc versus backarc attenuation of earthquake ground motion, *Bull. Seismol. Soc. Am.*, 101, 3032–3045.

Kurahashi, S, and K Irikura (2011). Source model for generating strong ground motions during the 2011 off the Pacific coast of Tohoku Earthquake, *Earth Planets Space*, 63, 571-576.

Meng, LS, A Inbal, and JP Ampuero (2011). A window into the complexity of the dynamic rupture of the 2011 Mw 9 Tohoku-Oki earthquake, *Geophys. Res. Lett.*, 38, L00G07, doi:10.1029/2011GL048118.

Nagumo, H. (2012), Rupture process of northern Nagano Prefecture earthquake on March 12th, 2011 (Mj6.7), Annual Meeting of Japan Association for Earthquake Engineering, Japan Association for Earthquake Engineering.

Skarlatoudis, A and CB Papazachos (2012). Preliminary study of the strong ground motions of the Tohoku, Japan, earthquake of 11 March 2011: Assessing the influence of anelastic attenuation and rupture directivity, *Seismol. Research Lett.*, 83, 119-129.

Stewart, JP, S Midorikawa, RW Graves, K Khodaverdi, T Kishida, H Miura, Y Bozorgnia, and KW Campbell (2013). Implications of Mw 9.0 Tohoku-oki Japan earthquake for ground motion scaling with source, path, and site parameters, *Earthquake Spectra*. Accepted.

Yokota, Y, K Koketsu, Y Fujii, K Satake, S Sakai, M Shinohara, and T Kanazawa (2011). Joint inversion of strong motion, teleseismic, geodetic, and tsunami datasets for the rupture process of the 2011 Tohoku earthquake, *Geophys. Res. Lett.* 38, L00G21, doi:10.1029/2011GL050098.

Zhao, JX, J Zhang, A Asano, Y Ohno, T Oouchi, T Takahashi, H Ogawa, K Irikura, HK Thio, PG Somerville, Y Fukushima, and Y Fukushima (2006). Attenuation relations of strong ground motion in Japan using site classification based on predominant period, *Bull. Seismol. Soc. Am.*, 96, 898–913.